Journal of Photochemistry and Photobiology A: Chemistry 274 (2014) 33–42

Contents lists available at ScienceDirect

Journal of Photochemistry and Photobiology A: Chemistry

journal homepage: www.elsevier.com/locate/jphotochem

Lactim–lactam tautomerism through four member hydrogen bonded network in isoindole fused imidazole system: A combined spectroscopic and theoretical approach to photophysical properties

Debarati Ray, Animesh Pramanik, Nikhil Guchhait*

Department of Chemistry, University of Calcutta, 92 A.P.C. Road, Calcutta 700009, India

ARTICLE INFO

Article history:
Received 3 May 2013
Received in revised form
30 September 2013
Accepted 3 October 2013
Available online 11 October 2013

Keywords:
1-(2-Hydroxy-5methyl-phenyl)-3,5-dioxo-1*H*-imidazo-[3,4-*b*]
isoindole
Lactim–lactam isomerization
Fluorescence
Density Functional Theory
ESIPT

ABSTRACT

This article presents the photophysical study of a pharmaceutically important isoindole fused imidazole derivative, namely 1-(2-hydroxy-5methyl-phenyl)-3,5-dioxo-1*H*-imidazo-[3,4-*b*] isoindole (ADII) using steady state absorption, emission and time resolved emission spectroscopy. The molecule possesses a four member intramolecular hydrogen bonded ring composed of O—H and N atom suitable for intramolecular proton transfer process. Absorption study of ADII suggests the existence of its lactim and lactam tautomeric form in the ground state. The appearance of large Stokes shifted emission signifies lactim–lactam isomerization by excited state proton transfer reaction. Quantum chemical calculations at Density Functional Theory (DFT) (B3LYP/6-311+G**) and Hartree–Fock (6-311+G**) levels have also been performed in support of the experimental findings. Both the level of theory suggests the existence of two tautomeric forms in the ground electronic state and the calculated potential energy surfaces along the proton transfer coordinate suggest the preference of excited state proton transfer reaction than the ground state with respect to activation barrier. The pH variance experiment is also carried out for investigating different absorbing and emitting species of ADII in aqueous and ACN medium.

1. Introduction

Among the various photoinduced intramolecular processes excited-state intramolecular proton transfer (ESIPT) process has been drawing great attention due to their ubiquitous application in various chemical and biological processes [1]. Numerous ESIPT molecules have been strategically designed and synthesized with an aim to understand the fundamental of proton transfer mechanism and/or to explore their potential applications in different directions [2–5]. Generally most of the ESIPT molecules possess a strong intramolecular hydrogen bonded six member ring between the donor O—H (or, N—H) and acceptor C=O (or, pyridinic N) groups. The close proximate acidic and basic moieties rearrange in an extremely fast period of time (within picoseconds) in the excited electronic state via a transfer of hydrogen or proton. ESIPT molecules are often characterized by dual emission: one corresponding to the normal emission, i.e., emission comes from the local excited (LE) state and the other large Stoke's shifted emission from the tautomeric species produced in the excited state.

This unique behavior of ESIPT phenomenon is widely applied in various fields such as: developments of ultraviolet stabilizers [6], laser dyes [7,8], radiation hard scintillators [9], LEDs [10], molecular energy storage [11], molecular switches [12] and molecular sensors [13], etc. Furthermore, the ESIPT phenomenon has been widely used as optical probes for the investigation of various biomimicking, biological and supramolecular microenvironments [14,15].

Structurally it is well known that under similar strength of proton donor/acceptor moieties, the strength of intramolecular hydrogen bonding is highest in case of six member system than five member system and least in case of four member one. For this reason intramolecular proton transfer (IPT) process in four member intramolecular hydrogen bonding system is very rare. The most popular and well studied molecule belonging to this class (i.e., four member intramolecular hydrogen bonding system) is 2-hydroxy pyridine (2HP) which remains in equilibrium between the two tautomeric forms: lactim form (i.e., the enol form 2-hydroxy pyridine (2HP)) and lactam form (i.e., the keto form 2-pyridone (2PY)) in the ground state. This two tautomeric pair present in substantial concentration at room temperature and the enthalpy change between the two forms (2HP and 2PY) is 2–3 kJ/mol in favor of the lactam form. A number of theoretical [16–19] and experimental [20–22] works have been done in order to explain the existence of two ground state tautomeric forms and the process of their interconversion. The most expected pathway related to this phenomenon is the direct proton transfer in the bare monomer. Theoretical calculation using DFT//B3LYP/6-311+G** method by considering IPT

* Corresponding author. Tel.: +91 33 2350 8386; fax: +91 33 2351 9755.
E-mail address: nguchhait@yahoo.com (N. Guchhait).

1010-6030/$ – see front matter © 2013 Elsevier B.V. All rights reserved.
http://dx.doi.org/10.1016/j.jphotochem.2013.10.001

approach reveals a high energy barrier (~2 eV) for lactim to lactam conversion in the ground state [23,24]. Hence, the reaction is thought to be mediated by the assistance of protic solvents through intermolecular hydrogen bonding which might lead to reduction of energy barrier compared to the monomer. A large volume of theoretical and experimental works have been done in order to investigate the role of various proton donor/acceptor solvents for the tautomerization reaction in 2HP system [25–28]. The ground state intramolecular proton transfer (GSIPT) phenomenon in 2HP was also explained by considering tunneling process as light hydrogen atom is involved in it. Borst et al. experimentally showed the contribution of tunneling process in the first excited singlet state of 2HP system [29]. Latter, Tautermann et al. have developed a reliable theoretical method for the determination of the ground state tunneling splitting in 2HP and generalized the method to molecular systems having symmetric double well type of potential [30]. Tunneling process has been successfully applied to various systems to explain the intrinsic intramolecular proton transfer behavior [5,31]. Double proton transfer model has also been proposed by many researchers to explain the tautomerization process of 2HP system [32]. Although DFT//B3LYP method fails to explain the experimental results of 2HP-2PY system, but this method has been quite appreciably used by several researchers to generate the potential energy surfaces (PES), barrier height etc. with commendable efficiency.

In the present work we have carried out detailed photophysical study of a synthesized heterocycles of isoindole fused imidazole bearing phenolic subunit, namely 1-(2-hydroxy-5methyl-phenyl)-3,5-dioxo-1*H*-imidazo-[3,4-*b*] isoindole (ADII) in order to understand its dual emissive behavior using simple spectroscopic technique. In medicinal chemistry, this type of heterocyclic compound is widely used as templates to design a variety of biologically active agents [33]. Generally imidazole-based heterocyclic molecules play an important role in various biochemical processes too [34–36]. It is important to note that the present compound ADII can be used successfully to stain human squamous epithelium cells particularly the nuclei [37]. Structurally the molecule having a four member intramolecular hydrogen bonding unit may be responsible for intramolecular proton transfer behavior. The spectral study of ADII is also interesting from the fundamental aspect of lactam–lactim tautomerisation process. Along with spectroscopic technique, quantum chemical calculations have also been performed in order to get a knowledge related to the stability of different conformers of ADII and viability of ground and excited state proton transfer process. The ground state structures of different conformers of ADII have been optimized using Density Functional Theory (DFT) and Hartree–Fock (HF) levels of theory and the excited state optimization has been performed only at Hartree–Fock (HF) level of theory. The ground and excited state potential energy curve (PEC) along the PT coordinate have been constructed to follow the possibility of the IPT process.

2. Experimental

2.1. Synthesis of ADII

A 1:3 mixture of ninhydrin (1.4 mmol) and p-cresol (4.2 mmol) was refluxed in AcOH until the adduct 2-hydroxy-2-(2¢-hydroxy-aryl)-1,3-indanediones (where aryl = 2-hydroxy-5-methyl-phenyl) was completely formed. The complete formation of the desired adduct was checked by TLC. Then urea (16.6 mmol) was added to the above reaction mixture and the mixture was refluxed for further 2.5 h. The reaction mixture turned into red color. Then the cold reaction mixture was poured into ice-cold water. A yellow solid product was filtered and purified by column chromatography over silica gel (petroleum ether/ethyl acetate, 70/30, v/v) to give our desired compound 1-(2-hydroxy-5methyl-phenyl)-3,5-dioxo-1*H*-imidazo-[3,4-*b*] isoindole. The compound was characterized by both ^{1}H and ^{13}C NMR spectroscopy and was crystallized from acetone. ^{1}H NMR (300 MHz, DMSO-d_6): δ 10.64 (bs, —NH), 7.80 (d, J = 7.8 Hz, 1H), 7.65 (t, J = 7.6 Hz, 1H), 7.47 (d, J = 7.6 Hz, 1H), 7.41–7.32 (m, 3H), 7.05 (d, J = 8.2 Hz, 1H), 6.96 (t, J = 7.5 Hz, 1H); ^{13}C NMR (75 MHz, DMSO-d_6): δ 157.4, 152.3, 144.5, 131.3, 129.1, 128.3, 127.8, 126.6, 124.2, 122.4, 119.0, 117.6, 116.4, 113.8, 113.4, 111.8.

2.2. Materials

Spectroscopic grade solvents such as acetonitrile (ACN), dioxane (DOX), methanol (MeOH), chloroform ($CHCl_3$) and methyl cyclohexane (MCH) were purchased from Spectrochem (India) and were used after proper distillation whenever required. Triply distilled water was used for the preparation of solutions. Trifluoroacetic acid (TFA) and triethyl amine (TEA) from Spectrochem were used as supplied. Sulfuric acid (H_2SO_4) and sodium hydroxide (NaOH) were obtained from E-Merck and were used as received.

2.3. Instrumentation and procedure

2.3.1. Steady-state spectral measurements

The absorption and emission measurements were performed on a Hitachi UV-Vis U-3501 spectrophotometer and Perkin-Elmer LS-55 fluorimeter, respectively. All the collected spectra were with appropriate background correction. Only freshly prepared solutions were used for spectroscopic study and all experiments were carried out at room temperature (300 K).

Fluorescence quantum yield (Φ_f) was determined using the following equation where β-naphthol (Φ_R = 0.23) in MCH is used as the secondary standard.

$$\Phi_S = \Phi_R \cdot \frac{A_S \cdot OD_R \cdot n_S^2}{A_R \cdot OD_S \cdot n_R^2} \quad (1)$$

Where, Φ_S and Φ_R are the quantum yields, A_S and A_R are the integrated fluorescence areas, OD_S and OD_R are the absorbance values and n_S and n_R are the refractive indices of sample and reference molecule, respectively.

2.3.2. Time-resolved fluorescence decay

Fluorescence lifetimes were obtained by the method of Time Correlated Single-Photon counting (TCSPC) on FluoroCube-01-NL spectrometer (Horiba Jobin Yovon) using light source of nano LED at 336 nm, 291 nm and laser source at 450 nm. The signals were collected at the magic angle of 54.7^o to eliminate any considerable contribution from fluorescence anisotropy decay. The decays were deconvoluted using DAS-6 decay analysis software and the acceptability of the fits was judged by χ^2 criteria and visual inspection of the residuals of the fitted function to the data. The time-resolved fluorescence decay ($I(t)$) is described by the following expression:

$$I(t) = \sum_i \alpha_i \tau_i \quad (2)$$

and the mean (average) fluorescence lifetimes are calculated using the following equation [38]:

$$\langle \tau_{i0} \rangle = \frac{\sum_i \alpha_i \tau_i^2}{\sum_i \alpha_i \tau_i} \quad (3)$$

in which α_i is the pre-exponential factor corresponding to the ith decay time constant, τ_i.

2.4. Theoretical calculations

All theoretical calculations were performed to evaluate the energies, preferred geometries and potential energy surfaces with the GUASSIAN 03 suit of program [38]. The ground state geometries of different conformers of ADII were optimized at Density Functional Theory (DFT) level of theory using B3LYP functional, while Hartree Fock (HF) method was employed for the optimization of the ground as well as excited state geometries. For both the level of theory 6-311+G** basis set have been used. The ground state potential energy curve (GS-PEC) has been constructed by using the energies of the fully optimized geometries (using DFT//B3LYP/6-311+G** method) of ADII at fixed O_d—H distance over the range 0.90–2.45 Å. For the excited state PEC, TDDFT method has been used to calculate the vertical excitation energy with the same B3LYP functional and 6-311+G** basis set. The obtained vertical excitation energy was then added to the corresponding GS-PEC to generate excited state potential energy curve. This approach of ground and excited state PEC generation is successfully applied in some recent theoretical calculations for the study of ESIPT reaction [38,40–42].

3. Results and discussion

3.1. Absorption study

Structurally ADII molecule has a common motif with the very popular 2-hydroxypyridine (2HP) system (similar part is marked by a circle in Scheme 1). Therefore, it is quite reasonable to expect the spectroscopic behavior of ADII molecule to be similar with 2HP system. In all solvents 2HP exhibits two absorption bands, one at the region of ~227–230 nm and another at ~297–305 nm [17,38]. These bands were assigned to the corresponding lactim (2HP) and lactam form (2PY) of 2-hydroxypyridine system. Recently, we have reported two analogous systems 2-hydroxy-5-(4-fluorophenyl) nicotinic acid (HEPNA) [38] and 5-(4-fluorophenyl)-2-hydroxypyridine (FP2HP) [39] which show similar type of absorption spectra in all solvents. HEPNA exhibits two absorption bands at ~250 nm and ~350 nm while FP2HP shows two bands at ~270 nm and ~320 nm. For both the cases the shorter and longer wavelength bands have been assigned to their lactim form and lactam form, respectively [38,39]. Therefore we can easily say that the present studied ADII molecule may exist in its two tautomeric forms (lactim and lactam) in the ground state.

The absorption spectra of ADII have been displayed in Fig. 1 and the corresponding spectral parameters are summarized in Table 1. As seen in Fig. 1, the absorption spectra of ADII in different solvents are comprised of three bands at ~280 nm, ~315–320 nm (broad band) and a small hump at ~395–400 nm. The hump at ~395–400 nm is not so prominent and hence we have deconvoluted

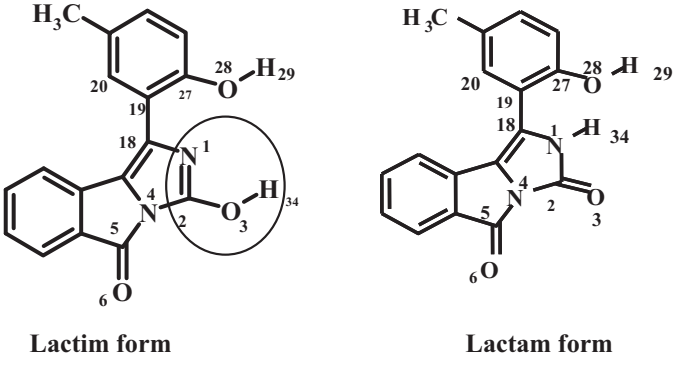

Scheme 1. Schematic presentation of ADII molecule (both lactim and lactam form).

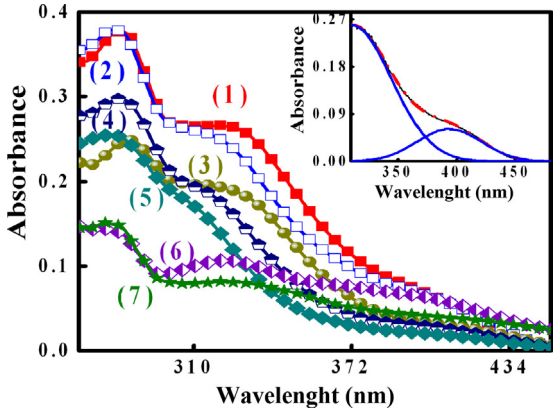

Fig. 1. Absorption spectra of ADII in different media (1 = DOX, 2 = ACN, 3 = DMSO, 4 = MeOH, 5 = Water, 6 = $CHCl_3$, 7 = MCH) at room temperature. Inset shows the resolved absorption spectra of ADII in ACN. The black lines denote the experimental spectra, the blue lines denote the resolved bands into the individual Lorentzian components and the red dashed lines designate the simulated spectra based on the resolved bands.

the absorption profile of ADII and is presented in the inset of Fig. 1. By comparing the absorption band of ADII with the previous reported analogous molecules, the bands at ~320 nm and ~395 nm have been assigned to the lactim and lactam-form of ADII, respectively. It is to mention here that the lactim form of ADII has two conformers: open form (IIa of Scheme 2) and closed form (IIb of Scheme 2) and theoretical calculation suggests that the closed form is more stable than the open form by 0.22 kcal/mol at DFT//B3LYP/6-311+G** level. As the calculated energy difference between the open and the closed form of lactim isomer is very less, we can say that the broad absorption band at ~320 nm (correspond to the lactim form) should consist of both the open and closed form of the lactim isomer. The red shift of both absorption bands of ADII is due to more aromatic stabilization of the molecule than the previously reported analogous systems. The high energy band appeared at ~280 nm may be due to $S_0 \rightarrow S_2$ type of electronic transition of the lactim form.

The solid state X-ray single crystal structure of ADII is unavailable in the literature but the crystal structure of its derivative has been reported by Das et al. [37]. Both ADII and its derivative are structurally identical at the hydrogen bonded ring site only with a little dissimilarity in the substitution on the phenolic subunit. From single crystal X-ray crystallographic study of the derivative [37] it is found that the lactam form of ADII is predominant in the solid state.

3.2. Emission and excitation study

The fluorescence spectra of ADII molecule have been recorded in various solvents including water and are presented in Fig. 2. As seen

Table 1
Spectroscopic parameters of ADII obtained from absorption and emission spectra in different solvents at room temperature.

Solvents	λ_{abs} (nm)	λ_{em} (nm)	Φ_f (λ_{ex} = 328 nm)
MCH	278, 325, 415	410, 480	0.36
$CHCl_3$	278, 320, 405	410, 470	0.38
ACN	280, 325, 405	415, 475	0.24
DOX	281, 325, 405	405, 470	0.40
DMSO	285, 323, 410	412, 487	0.22
iPrOH	282, 318, 410	410, 485	0.21
BuOH	280, 320, 410	410, 490	0.18
EtOH	280, 318, 405	415, 490	0.14
MeOH	280, 315, 405	415, 494	0.13
Water	278, 305, 405	423, 495	0.005

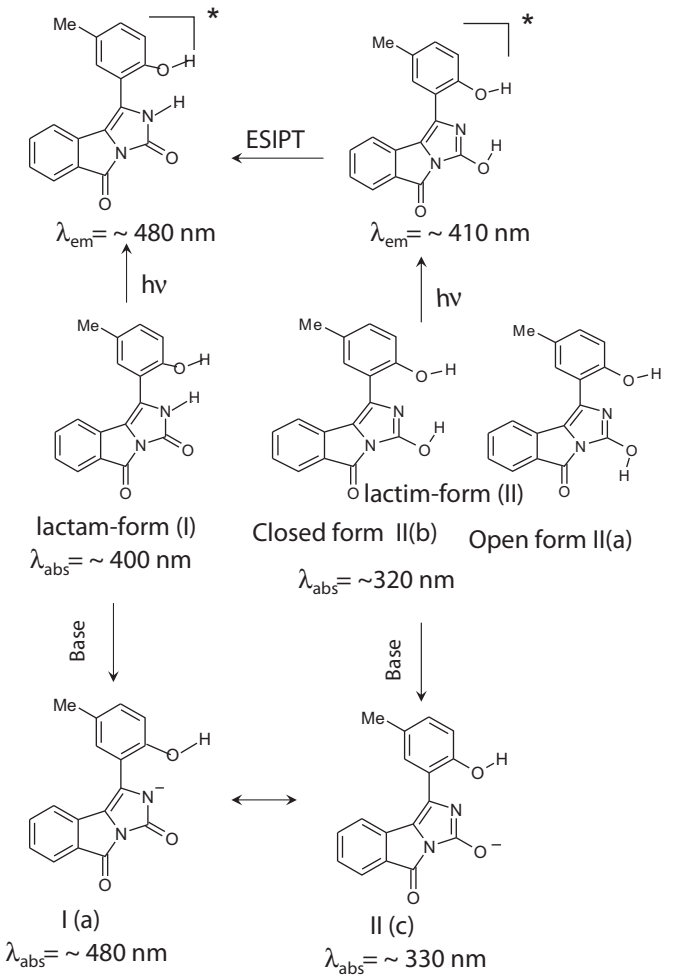

Scheme 2. Schematic presentation of ESIPT reaction (lactim–lactam tautomerism) and different absorbing and emitting species of ADII in variation of pH.

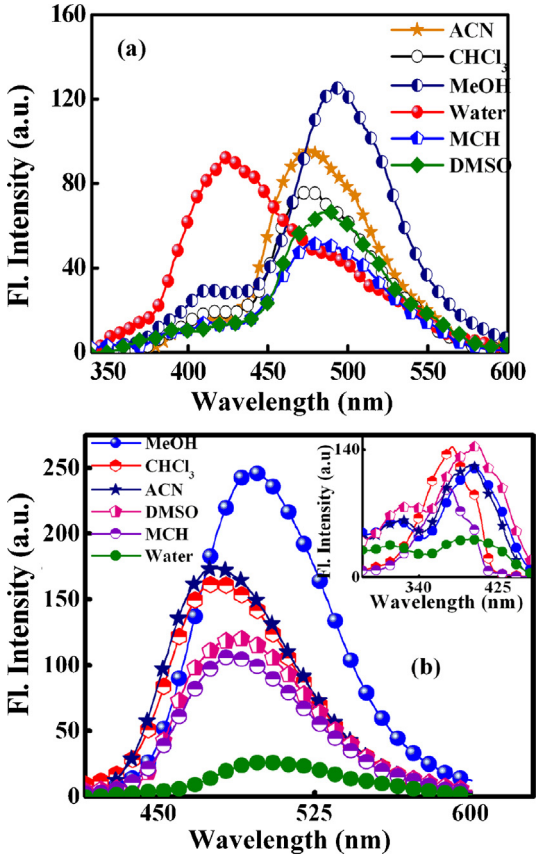

Fig. 2. Fluorescence emission spectra of ADII in different organic solvents at room temperature: (a) λ_{ex} = 320 nm, (b) λ_{ex} = 400 nm (inset shows the excitation spectra).

in Fig. 2a and b, in all solvents the molecule produces dual emission bands at ~410 nm and ~480 nm when excitation wavelength is set to 320 nm, whereas single emission at ~480 nm is observed when λ_{ex} is set to ~400 nm. Therefore, the band at ~480 nm is the local emission of lactam form of ADII which is also produced along with the lactim local emission (λ_{em} = ~410 nm) when excitation wavelength is set to 320 nm (at this wavelength only lactim form is excited). The observed dual emission upon photoexcitation of the lactim form suggests the operation of lactim to lactam isomerization by excited state proton transfer process. As the dual emission of ADII is observed in aprotic solvent also (here MCH), we can strongly infer that the proton transfer process in ADII is an intramolecular one and it does not need any assistance of protic solvents which is necessary for intermolecular proton transfer process.

The inset of Fig. 2b reveals that in all solvents the excitation spectra of ADII contain two bands: one at ~315 nm and another at ~390 nm when λ_{em}^{mon} = 480 nm. This result confirms that emission at 480 nm is composed of the both the LE of the lactam form and a part generated from the lactim to lactam isomerization by the operation of ESIPT process.

The emission spectral behavior of ADII is interestingly different in water in comparison with other organic solvents. In all other solvents the fluorescence intensity of PT band is much higher than that of the LE emission while the reverse phenomenon is observed in water when excited at 305 nm (only lactim form is excited). This behavior of ADII in water may imply that more stabilization of the lactim form through intermolecular hydrogen bonding interaction inhibits the formation of excited state tautomer. Time resolved emission data of ADII in water also supports the steady state findings which have been discussed in Section 3.5. The spectroscopic data presented in Table 1 also reveals that the longer wavelength emission band of ADII shows some solvent dependency. A red shifted emission of PT band is observed in hydrogen bonding solvents.

3.3. *Spectral modulations as a function of variation of medium-pH*

The variation of medium pH results some interesting modification on the absorption and emission spectral profile of ADII. As seen in Fig. 3a, ADII generates a new absorption band at ~485 nm and the absorption band of the lactam form at ~400 nm decreases its intensity upon addition of triethyl amine (TEA) in acetonitrilic solution. This new band is assigned to the anionic form (Ia of Scheme 2) which is generated from the deprotonation of N—H of the lactam form. A minute change in the absorption profile of ADII is noticed in presence of organic acid like trifluoro acetic acid (TFA) (Fig. 3b).

Different observations are found when base NaOH is added in aqueous medium of ADII. Fig. 4a shows that initially at very low concentration of NaOH (1.25×10^{-4} M) a new band is developed at ~450 nm which vanishes with increasing concentration of the base (7×10^{-3} M) with gradual development of a new band at ~330 nm. The band at ~330 nm must be the anionic form generated from the lactim form of ADII (IIc of Scheme 2) as the absorption band assigned for the lactim form is centered at ~320 nm. It is also note that the anionic species Ia is dominating in basic acetonitrilic medium while latter IIc is present in basic aqueous medium. The acid effect in aqueous medium of ADII (*vide* Fig. 4b) produces

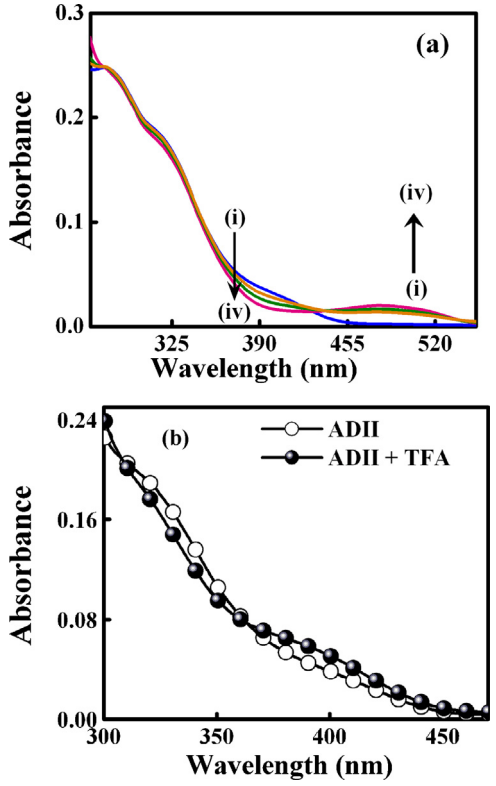

Fig. 3. Effect of addition of (a) base TEA where, spectra (i)→(iv) [TEA] = 0, 2.62×10^{-5}, 6.44×10^{-5}, 9.78×10^{-5} and 5.01×10^{-4} M and (b) acid TFA on the absorption profile of ADII in ACN.

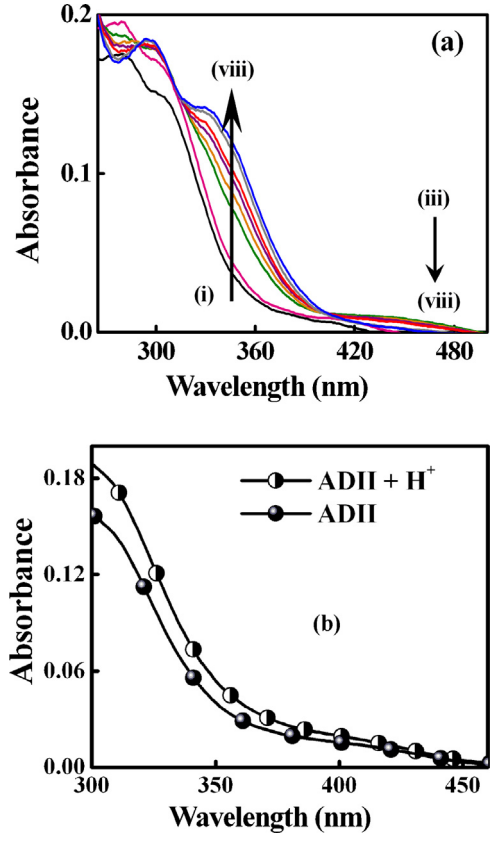

Fig. 4. Effect of addition of (a) base (NaOH), spectra (i)→(viii) [NaOH] = 0, 1.25×10^{-4}, 2.5×10^{-4}, 5.5×10^{-4}, 7.57×10^{-4}, 1.25×10^{-3}, 5.5×10^{-3} and 7×10^{-3} M and (b) acid (H_2SO_4) on the absorption spectra of ADII in aqueous medium.

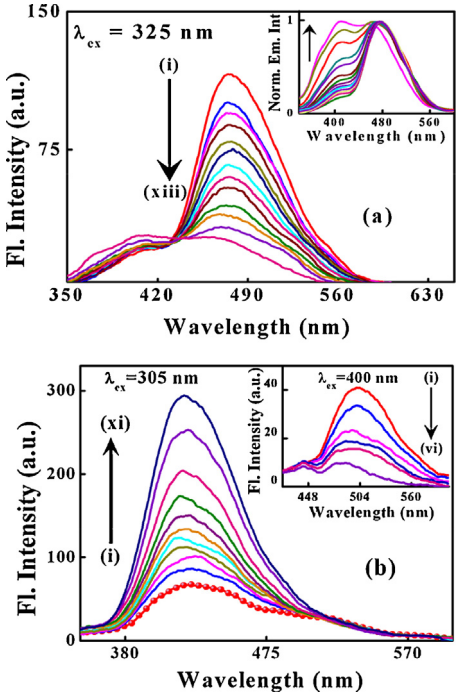

Fig. 5. Effect of base on the emission profile of ADII in (a) ACN medium (inset shows the normalized spectra of base effect in ACN medium), spectra (i)→(xiii) [TEA] = 0, 4.77×10^{-6}, 9.55×10^{-6}, 1.67×10^{-5}, 2.62×10^{-5}, 4.05×10^{-5}, 6.44×10^{-5}, 9.78×10^{-5}, 1.43×10^{-4}, 2.14×10^{-4}, 3.10×10^{-4}, 5.01×10^{-4} and 1.26×10^{-3} M and (b) aqueous medium spectra (i)→(xi) [NaOH] = 0, 2.75×10^{-5}, 6.87×10^{-5}, 1.23×10^{-4}, 1.92×10^{-4}, 3.02×10^{-4}, 4.95×10^{-4}, 8.25×10^{-4}, 1.1×10^{-3}, 1.65×10^{-3} and 6.6×10^{-3} M (inset shows the same at different excitation wavelength where, spectra (i)→(vi) [NaOH] = 0, 2.75×10^{-5}, 1.23×10^{-4}, 4.95×10^{-4}, 8.25×10^{-4}, 1.65×10^{-3} and 3.3×10^{-3} M).

similar results that were obtained by the treatment of TFA treatment on the acetonitrilic solution.

The modifications of emission profile of ADII upon increasing pH of the solution are also noteworthy. As seen in Fig. 5a, upon addition of organic base like TEA in ACN solution of ADII, the proton transfer (PT) band at 475 nm decreases with a blue shift of the emission maxima (shifted to 462 nm), but the modification of the lactim emission (λ_{max} = 405 nm) in presence of TEA is practically unclear. For better information regarding the aforesaid fact the entire emission profile is normalized at the PT band and is presented in the inset of Fig. 5a. It is found that LE band intensity enhances with a slight red shift from 405 nm to 410 nm. Similar kind of experiment has been done in aqueous solution of ADII. In presence of strong base like NaOH, the intensity of lactim emission at ~425 nm enhances with a slight blue shift of the emission maxima (shifted to ~420 nm), while the lactam emission (~500 nm) quenches with comparatively large blue shift of emission maxima to ~480 nm (Fig. 5b). These results infer that ESIPT mechanism is hampered due to the deprotonation (O—H_{34}) of lactim form in the basic medium. The red shifted band developed at ~410 nm in basic ACN medium or the blue shifted band at ~420 nm in basic aqueous solution is the same anionic species developed due to the deprotonation of lactim form (Ia of Scheme 2). Similarly, the band at ~480 nm and ~462 nm in the respective basic aqueous and ACN medium are also the anionic species originated from the lactam form (IIc of Scheme 2). On the other hand, as seen in Fig. 6a, with increasing acid concentration in the ACN medium of ADII the PT emission decreases with slight bathochromic shift (from 475 nm to 483 nm), but lactim emission is unchanged. In aqueous solution of ADII the emission profile shows reverse phenomena than that was observed in high pH condition, i.e., LE band decreases in presence of acid (Fig. 6b). The lowering of PT emission in acidic medium

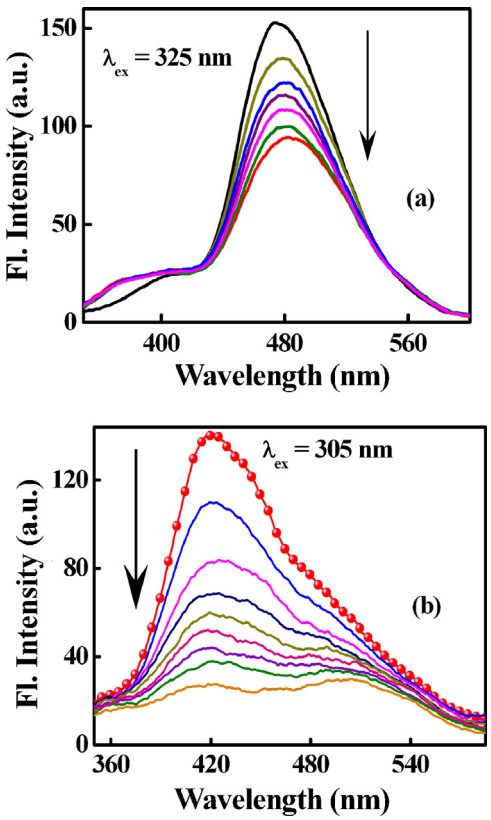

Fig. 6. Effect of acid on the emission profile of ADII in: (a) ACN medium and (b) aqueous medium.

is probably due to the protonation of lactim nitrogen of ADII which also hampers the ESIPT operation.

3.4. Fluorescence quantum yield measurements

The fluorescence quantum yields of ADII have been measured in different solvents of varying polarity using β-naphthol (Φ_R = 0.23) in MCH as the secondary standard. The fluorescence quantum yields of ADII at room temperature in different solvents are tabulated in Table 1. It is found that the magnitude of fluorescence quantum yield of ADII in polar protic solvents is lower than in other nonpolar aprotic solvents and for water this value is nearly hundred times lower than other solvents (even other protic solvents). This may be due to intermolecular hydrogen bonding interaction of ADII with protic solvents which activates various nonradiative channels.

3.5. Fluorescence lifetime measurements

The time-resolved fluorescence spectroscopy is a reliable tool to investigate the existence of different emitting species. The time resolved fluorescence spectra of ADII in different solvents at varying excitation wavelength are displayed in Fig. 7 and the corresponding time resolved fluorescence data are presented in Table 2. It is found that the time resolved data of ADII in water is completely different from the other organic solvents. The molecule has been excited at 450 nm and the fluorescence decays have been collected by setting the emission wavelength at 500 nm with an aim to excite only the lactam form (since lactim form does not absorb at this wavelength). The collected time resolved fluorescence data have been best fitted to single exponential function in all organic solvents and the corresponding time constant value (7.08 ns in ACN) is definitely the excited state lifetime of the lactam form of ADII. However, when λ_{ex} is set to 336 nm and λ_{em} is set to 385 nm (at this excitation wavelength only lactim form is excited and there is no contribution for the lactam form at this wavelength), the decay pattern follows triexponential function with time constant values of ~0.155 ns (83%), ~1.68 ns (11%) and ~5.32 ns (6%) in ACN solvent (time constant values and their relative populations of ADII in different solvents are mentioned in Table 2). During excitation at 336 nm we have preferentially excited the lactim form (both open and closed form) and the monitoring emission wavelength (here 385 nm) also shares a very minute overlapping zone with the lactam emission; therefore the obtained fluorescence decay at this excitation and emission wavelength may consist of the three species: open and closed form of lactim isomer and the lactam form of ADII. As the excited state lifetime of lactam form is 7.08 ns (in ACN, from the TCSPC data at λ_{ex} = 450 nm), the two other components of ~0.155 ns and ~1.68 ns definitely come from the excited lactim form (both open form and closed form). Moreover, a bi-exponential decay pattern with major contribution of (80%) slower component (6.86 ns in ACN) and a comparatively short lived (1.32 ns in ACN) minor component (20%) are also found when ADII is excited at 336 nm and emission wavelength is set to 500 nm (i.e. PT band). That upon selective excitation of the lactim form (λ_{ex} = 336 nm) the decay of the lactam form is observed due to the operation of ESIPT (lactim → lactam) process over the excited state potential energy surface (PES) and this observation strongly support our steady state spectral findings. As

Table 2
Fluorescence lifetimes of ADII in different solvents at room temperature.

Solvents	λ_{ex} (nm)	λ_{mon} (nm)	τ_1 (α_1) (ns)	τ_2 (α_2) (ns)	τ_3 (α_3) (ns)	$\langle\tau_{i0}\rangle$ (ns)	χ^2
MCH	336	385	1.78 (0.19)	4.4 (0.03)	0.205 (0.78)	1.93	1.03
	336	490	1.24 (0.14)	5.83 (0.86)	–	5.67	1.15
	450	490	–	4.43 (1)	–	4.43	1.1
$CHCl_3$	336	385	1.77 (0.28)	6.61 (0.05)	0.412 (0.67)	2.88	1.08
	336	490	0.63 (0.21)	5.19 (0.79)	–	5.04	1.1
	450	490	–	5.15 (1)	–	5.15	1.08
ACN	336	385	1.68 (0.11)	5.32 (0.06)	0.155 (0.83)	3.20	1.06
	291	385	2.18 (0.28)	6.72 (0.16)	0.371 (0.56)	4.56	1.06
	336	490	1.32 (0.21)	6.86 (0.79)	–	6.59	1.09
	450	490	–	7.08 (1)	–	7.08	1.2
MeOH	336	385	1.43 (0.06)	6.28 (0.009)	0.132 (0.92)	1.87	1.15
	291	385	1.52 (0.29)	6.49 (0.13)	0.361 (0.58)	4.16	1.10
	336	500	2.22 (0.32)	6.23 (0.68)	–	5.65	1.11
	450	500	–	5.56 (1)	–	5.56	1.2
Water	336	385	2.34 (0.05)	8.36 (0.05)	0.25 (0.90)	5.01	1.09
	336	500	2.09 (0.05)	8.24 (0.05)	0.019 (0.9)	6.77	1.07
	450	500	1.02 (0.04)	7.05 (0.02)	0.13 (0.94)	3.45	1.2

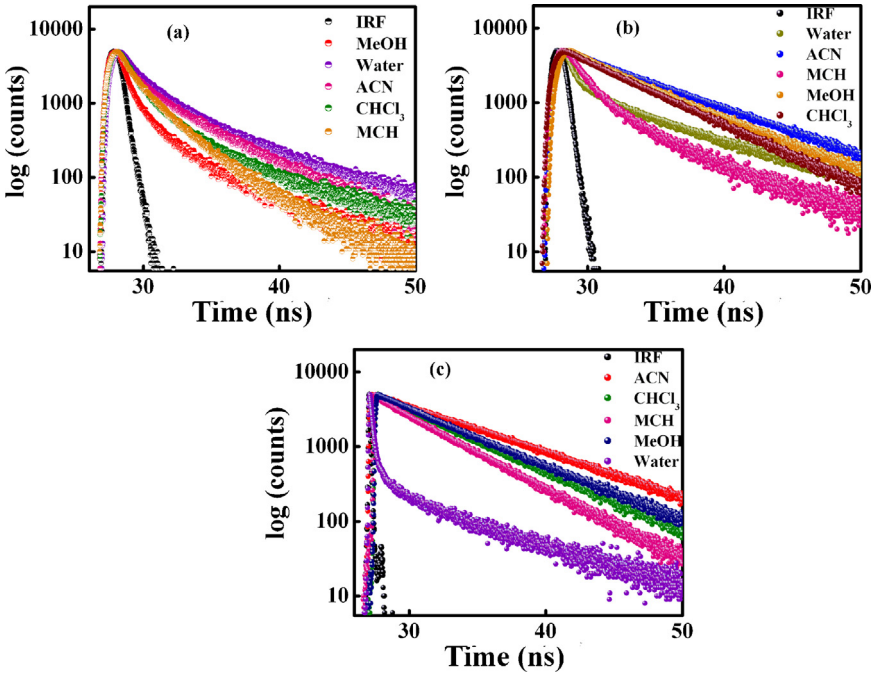

Fig. 7. Time-resolved emission decay profile of ADII in different solvents at different excitation wavelength at (a) λ_{ex} = 336 nm and λ_{mon} = 385 nm, (b) λ_{ex} = 336 nm and λ_{mon} = 490 nm and (c) λ_{ex} = 450 nm and λ_{mon} = 490 nm.

the close form of the lactim isomer undergoes ESIPT operation, 1.32 ns decay component is definitely the excited state lifetime of the closed form and the shortest time constant (0.155 ns in ACN, at λ_{ex} = 336 nm and λ_{em} = 385 nm) is undoubtedly arising from the excited open form of the lactim isomer.

It is interesting to note that the TCSPC results of ADII in water are widely different with respect to other organic solvents. In water, the time resolved data have been best fitted with tri-exponential function (for both λ_{ex} = 336 nm and 450 nm) with dominating contribution (>90%) of faster component (0.019 ns when λ_{ex} = 336 nm and 0.13 ns for λ_{ex} = 450 nm) along with two other very minor components (7.05 and 1.02 ns, each 5%). Thus the very poor excited state population of the lactam form strongly infers that ESIPT operation of ADII is hampered in water and this result is also reflected in the steady state emission profile by a low emission intensity of PT band in comparison to the LE band.

Table 3
Relevant structural parameters for the optimized ground and excited state ADII at HF and CIS levels and at DFT level with B3LYP hybrid functional and 6-311+G** basis set.

Molecular parameters[a]	Calculated data					Crystal data of the lactam form
	HF level			DFT level/B3LYP		
	Lactim-form		Lactam-form	Lactim-form	Lactam-form	
	GS	ES	GS	GS	GS	
Bond length (Å)						
N1—H34	2.38	2.38	0.99	2.39	1.007	0.881
C2—O3	1.31	1.31	1.18	1.33	1.20	1.222
O3—H34	0.94	0.95	2.62	0.97	2.67	2.609
N1—C2	1.28	1.32	1.37	1.30	1.39	1.368
C2—N4	1.35	1.33	1.41	1.37	1.41	1.391
N4—C5	1.40	1.42	1.42	1.43	1.42	1.411
C5—O6	1.18	1.19	1.20	1.20	1.20	1.215
O28—H29	0.94	0.94	0.96	0.96	0.96	0.83
O28—H34	–	–	2.22	–	2.22	2.24
Angle and dihedral angle (°)						
∠H34—N1—C2	50.15	50.46	121.33	50.45	122.05	123.00
∠N1—C2—O3	126.77	125.02	127.82	126.71	128.03	127.82
∠C2—O3—H34	108.42	109.28	49.95	106.93	49.73	49.95
∠C2—N4—C5	140.85	141.36	136.29	141.06	136.29	136.94
∠N4—C5—O6	126.98	125.16	126.94	126.25	126.94	125.52
∠H34—N1—C2—O3	0.44	0.70	12.03	0.53	9.57	4.06
∠N1—C2—O3—H34	−0.91	−1.42	−5.04	−1.05	−3.98	1.57
∠C2—N4—C5—O6	2.53	2.55	4.88	4.146	4.89	1.46
∠N1—C18—C19—C20	−115.87	−128.92	−133.39	−128.99	−144.70	−146.38
∠N1—C18—C19—C27	64.23	51.84	34.13	51.41	34.16	31.15

[a] The numbering of the various atoms mentioned in Table 3 is presented in Scheme 1.

3.6. Quantum chemical calculations

We have earlier mentioned that the crystal structure of ADII is unavailable but the crystal structure of its derivative is available in the literature. Both ADII and its derivative are structurally identical with a little dissimilarity in the substitution on the phenolic subunit. The single crystal X-ray analysis of the derivative of ADII reveals the predominance of lactam form in the solid state. The geometry obtained from X-ray diffraction data of its derivative with proper correction to the substitution of the phenolic subunit was used as the input file for the full geometry optimization purpose. The ground state (GS) geometry of ADII has been optimized at both Density Functional Theory (DFT) and HF level using B3LYP hybrid functional and 6-311+G** basis set. The obtained structural parameters from the above mentioned level of theory and the available crystallographic studies are presented in Table 3 to verify the reliability of our theoretical calculation. Both the single crystal X-ray analysis and optimized geometry of ADII reveals that three fused rings are in the same plane and the phenolic subunit remains out of plane with dihedral angle of −146.38° and the hydrogen atom of the phenolic O—H group remains out ward. From both the level of calculations (DFT and HF) it is clear that in the GS (in vacuo) lactam form is more stable than the lactim form with an energy difference between the two forms is 15.68 kcal/mol (according to DFT level and using HF level this value is 13.62 kcal/mol) and the closed conformer of lactim form is more stable than the open conformer by 0.22 kcal/mol (according to DFT level and using HF level this value is 0.98 kcal/mol).

All the previous discussion based on the steady state and time resolved fluorescence study suggests the intrinsic ESIPT behavior of ADII. Here also, from the optimization of the excited state geometry of the lactim form using HF level of theory, it is found that O_3—H_{34} bond length increases from 0.944 Å (in GS) to 0.945 Å (in ES) and also C_2—O_3 bond distance decreases from 1.31 Å (in GS) to 1.30 Å (in ES). In addition to the change in bond length in the ES optimized structure, Mulliken charge distribution over the atoms (i.e., atoms in lactim form) involved in the intramolecular proton transfer process also change remarkably which again supports our experimental findings. The respective negative and positive charge (Mulliken) densities over N and H atoms increase from −0.149 (in GS) to −0.18 (ES) and from 0.312 (in GS) to 0.315 (ES), respectively. NBO charge calculation has also been performed on the optimized ground and excited state geometry of the lactim form. The negative and positive NBO charge densities over the N and H atom increase from −0.544 (in GS) to −0.633 (in ES) and 0.495 (in GS) to 0.498 (in ES), respectively. These data provide a strong support in favor of the translocation proton (here H_{34} in Scheme 1) of the lactim form upon photo excitation.

The PECs of ADII in the ground and the first excited singlet state have been constructed by considering the ESIPT approach and are presented in Fig. 8a. The distance between the transferable proton (H_{34}) from O_3 atom (from where the H_{34} gets detached for its association with N_1 to generate the lactam form) has been taken as independent reaction coordinate (RC) and the PECs have been constructed by observing the change of energy along the RC [38,40,41,43]. The $R_{O3–H34}$ bond distance was varied from 0.90 to 2.45 Å with 0.05 Å increment and for each choice of O_3—H_{34} distance the rest of geometry was optimized. The simulated ground and excited state PECs generated for ADII molecule (considering ESIPT mechanism) are found to be very similar with its parent 2HP-2PY system and its analogous compound HEPNA [17,38]. Both the ground and excited states PECs are comprised of double well minima: one corresponding to the lactim and other for the lactam form. In the GS lactam form is energetically more stable than the lactim form by an energy difference of 15.68 kcal/mol (in vacuo). It

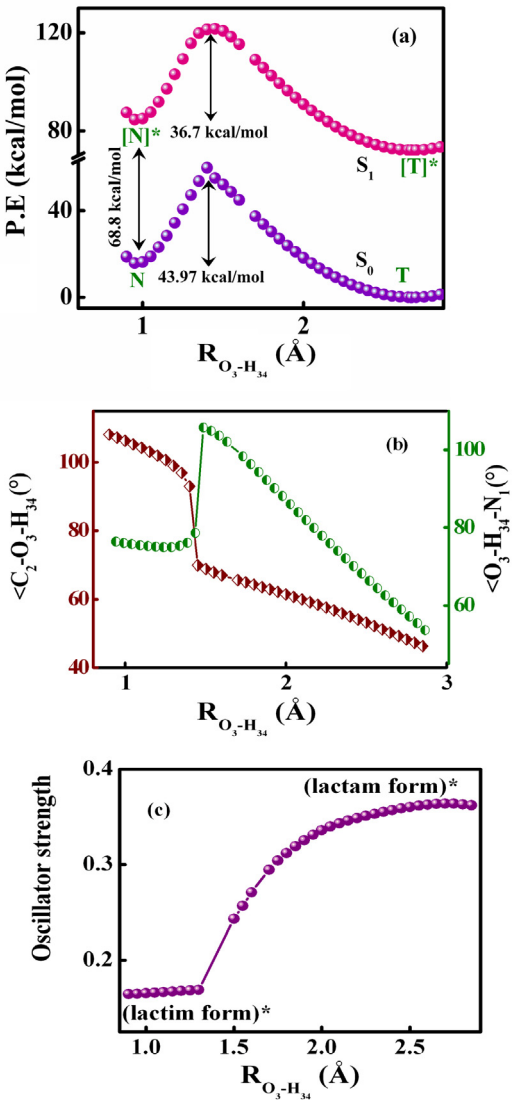

Fig. 8. (a) Potential energy curves for S_0 and S_1 states of ADII molecule, the variation of (b) $\angle C_2$—O_3—H_{34} and $\angle O_3$—H_{34}—N_1 and (c) the oscillator strength in the S_1 state along the proton transfer coordinate (O_3—H_{34} bond axis). The calculations are carried over at DFT//B3LYP/6-31G** level for the S_0 state and at the TDDFT (TD-B3LYP/6-31G**) level for S_1 state.

can be also seen in Fig. 8a that the ground state activation energy (E_{act}) for the ESIPT process is 1.89 eV whereas the same in the first excited singlet state (S_1) decreases to 1.58 eV. This result indicates more feasibility of IPT process in the excited state than the ground state. These two E_{act}s are quite high using DFT//B3LYP/6-311+G** method, but these results are in the same line with the other reported compounds like HEPNA and parent 2HP-2PY system [17,38]. During the process of proton transfer process other geometrical parameters like $\angle C_2$—O_3—H_{34} and $\angle O_3$—H_{34}—N_1 angles are significantly modulated along the RC ($R_{O3–H34}$). Fig. 8b depicts the variation of these two angles with the proton transfer coordinates ($R_{O3–H34}$), reflecting the intrinsic complex nature of the phenomenon.

The variation of oscillator strength with $R_{O3–H34}$ distance (i.e., on going from lactim-form to the lactam-form) in the S_1 state is presented in Fig. 8c. Enhancement of the calculated oscillator strength from lactim-form to the lactam-form on the S_1 surface implies the high fluorescence quantum yield of the proton transferred species (lactam-form).

4. Conclusion

In this article, the photophysical properties of ADII have been investigated using steady state absorption, emission and time resolved fluorescence spectroscopy. In all solvents the molecule shows dual emission due to an efficient intramolecular proton transfer reaction where lactim form of ADII converts to its corresponding lactam form. Absorption study also confirms the existence of lactim and lactam form in the ground state in all solvents. Steady state and time resolved fluorescence measurements suggest that ESIPT operation in ADII is less favorable in water than in other organic solvents.

Theoretical calculations using DFT and HF level of theory have also been carried out to support the experimental findings. The Mulliken and NBO charge distribution analysis over the atoms involved in the ESIPT process suggests the possibility of ESIPT operation. The ground and excited state PECs are comprised of two minima: one corresponding to lactim form and the other for lactam form. The energy barrier of lactim → lactam change over decreases in the excited state but the value is still very high using DFT//B3LYP/6-311+G** method. From the fundamental view point searching for an ESIPT process with a well defined energy barrier is of great interest to investigate the dynamics of hydrogen bond. Therefore we are optimistic that our system could be an ideal model for probing ESIPT dynamics and would be a great theoretical challenge.

Acknowledgments

DR acknowledges the University Grant Commission, Govt. of India for research fellowship. NG acknowledges the Department of Science and Technology, Govt. of India (Project No. SR/S1/PC/26/2008) and UPE Laser group for financial assistance.

References

[1] For instance: Studies in physical and theoretical Chemistry A. Müller, H. Ratajack, W. Junge, E. Diemann (Eds.), Electron and Proton Transfer in Chemistry and Biology, Elsevier, Amsterdam, 1992.
[2] S. Scheiner, Theoretical studies of excited state proton transfer in small model system, J. Phys. Chem. A 104 (2000) 5898–5909.
[3] J. Waluk, Conformational aspects of intra- and intermolecular excited-state proton transfer, in: J. Waluk (Ed.), Conformational Analysis of Molecules in Excited States, Wiley-VCH, New York, 2000.
[4] M.J. Paterson, M.A. Robb, L. Blancafort, A.D. DeBellis, Theoretical study of benzotriazole UV photostability: ultrafast deactivation through coupled proton and electron transfer triggered by a charge-transfer state, J. Am. Chem. Soc. 126 (2004) 2912–2922.
[5] W.-S. Tu, C.-C. Cheng, Y.-M. Cheng, P.-C. Wu, Y.-H. Song, Y. Chi, P.-T. Chou, Excited-state intramolecular proton transfer in five-membered hydrogen-bonding system: 2-pyridyl pyrazoles, J. Am. Chem. Soc. 125 (2003) 10800–10801.
[6] J. Catalan, F. Fabero, M.S. Guijarro, R.M. Claramunt, M.D.S. Maria, M.C. FocesFoces, F.H. Cano, J. Elguero, R. Sastre, Photoinduced intramolecular proton transfer as the mechanism of ultraviolet stabilizers: a reappraisal, J. Am. Chem. Soc. 112 (1990) 747–759.
[7] P. Chou, D. McMorrow, T.J. Aartsma, M. Kasha, The proton-transfer laser. Gain spectrum and amplification of spontaneous emission of 3-hydroxyflavone, J. Phys. Chem. 88 (1984) 4596–4599.
[8] A.U. Acuna, A. Costela, J.M. Munoz, A proton-transfer laser, J. Phys. Chem. 90 (1986) 2807–2808.
[9] R.M. Tarkka, X. Zhang, S.A. Jenekhe, Electrically generated intramolecular proton transfer: electroluminescence and stimulated emission from polymers, J. Am. Chem. Soc. 118 (1996) 9438–9439.
[10] P. Chou, D. McMorrow, T.J. Aartsma, M. Kasha, The proton-transfer laser gain spectrum and amplification of spontaneous emission of 3-hydroxyflavone, J. Phys. Chem. 88 (1984) 4596–4599.
[11] T. Nishiya, S. Yamauchi, N. Hirota, M. Baba, I. Hanazaki, Fluorescence studies of intramolecularly hydrogen-bonded o-hydroxyacetophenone, salicylamide, and related molecules, J. Phys. Chem. 90 (1980) 5730–5735.
[12] G. Zhang, H. Wang, Y. Yu, F. Xiong, G. Tang, W. Chen, Diamond photodetector response to deep UV excimer laser excitation, Appl. Phys. B: Lasers Opt. 76 (2003) 677–681.
[13] Y. Wu, X. Peng, J. Fan, S. Gao, M. Tian, J. Zhao, S. Sun, Fluorescence sensing of anions based on inhibition of excited-state intramolecular proton transfer, J. Org. Chem. 72 (2007) 62–70.
[14] A. Stynik, M. Kasha, Excited-state intramolecular proton transfer as a fluorescence probe for protein binding-site static polarity, Proc. Natl. Acad. Sci. U. S. A. 91 (1994) 8627–8630.
[15] T. Ozturk, A.S. Klymchenko, A. Capan, S. Oncul, S. Cikrikci, S. Taskiran, B. Tasan, F.B. Kaynak, S. Ozbey, A.P. Demchenko, New 3-hydroxyflavone derivatives for probing hydrophobic sites in microheterogeneous systems, Tetrahedron 63 (2007) 10290–10299.
[16] C. Krebs, H.J. Hofmann, H.J. Kohler, C. Weiss, Problems concerning the theoretical treatment of tautomeric equilibria of hetrocycles, Chem. Phys. Lett. 69 (1980) 537–539.
[17] M.J. Scanlan, I.H. Hillier, A.A. MacDowell, Theoretical studies of the tautomeric equilibriums and isomer energetics of 2-, 3-, and 4-hydroxypyridine, J. Am. Chem. Soc. 105 (1983) 3568.
[18] A.L. Sobolewski, L. Adamowicz, Photophysics of 2-hydroxypyridine: an *ab initio* study, J. Phys. Chem. 100 (1996) 3933–3941.
[19] P.T. Chou, C.Y. Wei, F.T. Hung, Conjugated dual hydrogen bonds mediating 2-pyridone/2-hydroxypyridine tautomerism, J. Phys. Chem. B 101 (1997) 9119–9126.
[20] P. Beak, F.S. Fry Jr., J. Lee, F. Steele, Equilibration studies. Protomeric equilibria of 2- and 4-hydroxypyridines, 2- and 4-hydroxypyrimidines, 2- and 4-mercaptopyridines, and structurally related compounds in the gas phase, J. Am. Chem. Soc. 98 (1976) 171–179.
[21] O. Bensaude, M. Chevrier, J.-E. Dubois, Lactim/lactam tautomeric interconversion mechanism in water/polar aprotic solvent water systems. 2. Hydration of 2-hydroxypyridines. Evidence for a bifunctional water-catalyzed proton transfer, J. Am. Chem. Soc. 101 (1979) 2423–2429.
[22] L.D. Hatherley, R.D. Brown, P.D. Godfrey, A.P. Pierlot, W. Caminati, D. Damiani, S. Merlandi, L.B. Favero, Gas-phase tautomeric equilibrium of 2-pyridinone and 2-hydroxypyridine by microwave spectroscopy, J. Phys. Chem. 97 (1993) 46–51.
[23] Y. Matsuda, T. Ebata, N. Mikami, IR-UV double-resonance spectroscopic study of 2-hydroxypyridine and its hydrogen-bonded clusters in supersonic jets, J. Phys. Chem. A 105 (2001) 3475–3480.
[24] M.K. Hazra, T. Chakraborty, 2-Hydroxypyridine ↔ 2-pyridone tautomerization: catalytic influence of formic acid, J. Phys. Chem. A 110 (2006) 9130–9136.
[25] A. Held, D.W. Pratt, Hydrogen bonding in water complexes. Structures of 2-pyridone-H_2O and 2-pyridone-$(H_2O)_2$ in their S_0 and S_1 electronic states, J. Am. Chem. Soc. 115 (1993) 9708–9717.
[26] A. Held, D.W. Pratt, Ammonia as a hydrogen bond donor and acceptor in the gas phase. Structures of 2-pyridone-NH_3 and 2-pyridone-$(NH_3)_2$ in their S_0 and S_1 electronic states, J. Am. Chem. Soc. 115 (1993) 9718–9723.
[27] A. Dkhissi, R. Ramaekers, L. Houben, L. Adamowicz, G. Maes, DFT/B3-LYP study of the hydrogen-bonding cooperativity: application to $(2\text{-pyridone})_2$, 2-pyridone-H_2O, 2-pyridone-CH_3OH and 2-pyridone-CH_3OCH_3, Chem. Phys. Lett. 331 (2000) 553–560.
[28] A. Maris, P. Ottaviani, W. Caminati, Pure rotational spectrum of 2-pyridone water and quantum chemical calculations on the tautomeric equilibrium 2-pyridone water/2-ydroxypyridine water, Chem. Phys. Lett. 360 (2002) 155–160.
[29] D.R. Borst, J.R. Roscioli, D.W. Pratt, G.M. Florio, T.S. Zwier, A. Müuller, S. Leutwyler, Hydrogen bonding and tunneling in the 2-pyridone 2-hydroxypyridine dimer. Effect of electronic excitation, Chem. Phys. 283 (2002) 341–351.
[30] C.S. Tautermann, A.F. Voegele, K.R. Liedl, The ground state tunneling splitting of the 2-pyridone·2-hydroxypyridine dimer, Chem. Phys. 292 (2003) 47–52.
[31] H. Rostkowska, L. Lapinski, A. Khvorostov, M.J. Nowak, Proton transfer processes in selenourea: UV-induced selenone→selenol photoreaction and ground state selenol→selenone proton tunneling, Chem. Phys. 298 (2004) 223–232.
[32] M. Meuwly, A. Muller, S. Leutwyler, Energetics, dynamics and infrared spectra of the DNA base-pair analogue 2-pyridone·2-hydroxypyridine, Phys. Chem. Chem. Phys. 5 (2003) 2663–2672.
[33] A.F. Pozharskii, A.T. Soldatenkov, A.R. Katritzky, Heterocycles in Life and Society, John Wiley and Sons Ltd., New York, 1997.
[34] E.A. Barnard, W.D. Stein, The roles of imidazole in biological systems, Adv. Enzymol. Relat. Subj. Biochem. 20 (1958) 51–110.
[35] M. Boiani, M. Gonzalez, Imidazole and benzimidazole derivatives as chemotherapeutic agents, Mini-Rev. Med. Chem. 5 (2005) 409–424.
[36] Z. Jin, Muscarine, imidazole, oxazole and thiazole alkaloids, Nat. Prod. Rep. 22 (2005) 196–229.
[37] S. Das, R. Fröhlich, A. Pramanik, Synthesis and fluorescent properties of a new class of heterocycles of isoindole fused imidazoles with phenolic subunits, Org. Lett. 8 (2006) 4263–4266.
[38] B.K. Paul, A. Samanta, S. Kar, N. Guchhait, Lactim–lactam tautomerism is favoured over enol–keto tautomerism in 2-hydroxy-5-(4-fluorophenyl)nicotinic acid: experimental and quantum chemical approach, J. Photochem. Photobiol. A: Chem. 214 (2010) 203–214.
[39] M.J. Frisch, G.W. Trucks, H.B. Schlegel, G.E. Scuseria, M.A. Robb, J.R. Cheeseman Jr., J.A. Montgomery, T. Vreven, K.N. Kudin, J.C. Burant, J.M. Millam, S.S. Iyengar, J. Tomasi, V. Barone, B. Mennucci, M. Cossi, G. Scalmani, N. Rega, G.A. Petersson, H. Nakatsuji, M. Hada, M. Ehara, K. Toyota, R. Fukuda, J. Hasegawa, M. Ishida, T. Nakajima, Y. Honda, O. Kitao, H. Nakai, M. Klene, X. Li, J.E. Knox, H.P. Hratchian, J.B. Cross, C. Adamo, J. Jaramillo, R. Gomperts, R.E. Stratmann, O. Yazyev, A.J. Austin, R. Cammi, C. Pomelli, J.W. Ochterski, P.Y. Ayala, K. Morokuma, G.A.

Voth, P. Salvador, J.J. Dannenberg, V.G. Zakrzewski, S. Dapprich, A.D. Daniels, M.C. Strain, O. Farkas, D.K. Malick, A.D. Rabuck, K. Raghavachari, J.B. Foresman, J.V. Ortiz, Q. Cui, A.G. Baboul, S. Clifford, J. Cioslowski, B.B. Stefanov, G. Liu, A. Liashenko, P. Piskorz, I. Komaromi, R.L. Martin, D.J. Fox, T. Keith, M.A. Al-Laham, C.Y. Peng, A. Nanayakkara, M. Challacombe, P.M.W. Gill, B. Johnson, W. Chen, M.W. Wong, C. Gonzalez, J.A. Pople, Gaussian 03, Revision C.01, Gaussian, Inc., Wallingford, CT, 2004.

[40] R.B. Singh, S. Mahanta, S. Kar, N. Guchhait, Photo-physical properties of 1-hydroxy-2-naphthaldehyde: a combined fluorescence spectroscopy and quantum chemical calculations, Chem. Phys. 331 (2007) 373.

[41] A. Samanta, B.K. Paul, S. Kar, N. Guchhait, Excited state lactim to lactam type tautomerization reaction in 5-(4-fluorophenyl)-2-hydroxypyridine: spectroscopic study and quantum chemical calculation, J. Fluoresc. 21 (2011) 95–104.

[42] R. de Vivie-Riedle, V.D. Waele, L. Kurtz, E. Riedle, Ultrafast excited-state proton transfer of 2-(2′-hydroxyphenyl)benzothiazole: theoretical analysis of the skeletal deformations and the active vibrational modes, J. Phys. Chem. A 107 (2003) 10591–10599.

[43] A.L. Sobolewski, W. Domcke, Ab initio study of excited-state intramolecular proton dislocation in salicylic acid, Chem. Phys. 232 (1998) 257–265.